JOURNAL OF Applied Polymer SCIENCE

Microwave Absorption Enhancement of Fe_3O_4/Polyaniline Core/Shell Hybrid Microspheres with Controlled Shell Thickness

Bin Zhang, Yunchen Du, Peng Zhang, Hongtao Zhao, Leilei Kang, Xijiang Han, Ping Xu
Department of Chemistry, Harbin Institute of Technology, Harbin 150001, China
Correspondence to: Y. Du (E-mail: yunchendu@yahoo.com.cn); P. Xu (E-mail: pxu@hit.edu.cn)

ABSTRACT: Synthesis of Fe_3O_4/polyaniline (PANI) core/shell hybrid microspheres through an *in situ* polymerization route with the 300 nm Fe_3O_4 microspheres as the cores and nucleation sites for PANI is reported. PANI shell thickness, from 30 nm to 120 nm, can be controlled by modulating the weight ratio of aniline monomer and Fe_3O_4 microspheres. Fe_3O_4 microspheres that are actually comprised of many small nanoparticles display super paramagnetic feature, which has been maintained in Fe_3O_4/PANI core/shell hybrid materials. Fe_3O_4/PANI core/shell hybrid materials have enhanced microwave absorption than both the Fe_3O_4 microspheres and PANI, where a maximum reflection loss of −37.4 dB at 15.4 GHz has been reached from the sample with a PANI shell thickness of 100 nm. Introduction of dielectric loss, interfacial loss, and improved impedance from coating the Fe_3O_4 microspheres with PANI should account for the improved microwave absorption properties of the prepared Fe_3O_4/PANI core/shell hybrid materials. © 2013 Wiley Periodicals, Inc. J. Appl. Polym. Sci. 130: 1909–1916, 2013

KEYWORDS: conducting polymers; nanoparticles; nanowires and nanocrystals; thermogravimetric analysis; X-ray

Received 25 November 2012; accepted 25 March 2013; Published online 10 May 2013
DOI: 10.1002/app.39332

INTRODUCTION

Rapid development in telecommunications, digital and electronic systems, and fast processors has brought great concerns about electromagnetic interference (EMI) issues.[1,2] In order to eliminate or at least reduce the harmful EMI to human beings, a variety of materials have been used microwave absorbers over the past decade,[3–7] which can absorb electromagnetic (EM) waves effectively by converting the EM energy into thermal energy or dissipating the EM waves through interference. To date, microwave absorbers are required to possess the characteristics of high efficiency, light weight, small thickness, and wide frequency range response.[8–10]

Magentic materials, with magnetic loss features, have been realized as an very important component in microwave absorbers. However, pure magnetic metals like Co and Ni usually possess very limited microwave absorptions in the range of 1–18 GHz,[11–14] where their high densities also betray the diea of light weight microwave absorbers. Magnetite (Fe_3O_4), with unique magnetic features, is an important functional material that has been widely used as microwave absorbers with low cost and strong EM wave absorption.[15–17] In our previous study, we found the prepared porous Fe_3O_4 flower-like nanostructures can break through the Snoek's limit and show strong absorption at the GHz frequency range.[18] However, Fe_3O_4 suffers from easy oxidation and narrow absorption band, and thus core/shell structures with Fe_3O_4 as the core are widely developed as potential candidates with broadband microwave absorption. Recently, Fe_3O_4/TiO_2,[19,20] Fe_3O_4/SnO_2,[21] Fe_3O_4/ZnO,[22] $Fe_3O_4/Fe/SiO_2$,[23] and Fe_3O_4/C[24] core/shell structures are successfully prepared, which show promising EM wave absorption performances at the GHz range.

In order to meet further requirements of broadband microwave absorbers, the concept of combining both magnetic loss and dielectric loss has been extensively studied.[19] Conducting polymers, such as polyaniline (PANI) and polypyrrole (PPy), with excellent chemical stability, have been recognized as suitable dielectric media in EM wave absorption applications.[25–28] Nanocomposites with Fe_3O_4 core and conducting polymer shell, such as Fe_3O_4Poly(3,4-ethylenedioxythiophene),[29] Fe_3O_4/PPy,[30] have been demonstrated with sound electromagnetic properties. In the past few years, it has been widely reported that embedding the magnetic particles (ferrites, Ni, etc.) in conducting polymer matrices can lead to enhanced EM wave absorption and wider responsive frequency range.[31–34] Conducting polymers hybridized with carbon materials are also found to be good candidates as EMI and microwave absorption materials.[28,35]

Additional Supporting Information may be found in the online version of this article.

In this study, we demonstrated the successful preparation of core/shell Fe_3O_4/PANI hybrid microspheres through an *in situ* polymerization technique. The shell thickness of the conducting polymer can be well controlled by modulating the weight ratio of aniline monomer and Fe_3O_4 microspheres, and the EM wave absorption properties can be greatly changed by the shell thickness (amount of PANI). It is realized that the introduction of PANI can largely enhance the dielectric loss properties and improve the matching impedance of the hybrids, and thus leads to enhanced EM wave absorption performances. The obtained Fe_3O_4/PANI hybrid materials show improved microwave absorption properties than the reported magnetic core/conducting polymer shell hybrid materials.[32–34]

EXPERIMENTAL

Synthesis of Fe_3O_4 Microspheres

Fe_3O_4 microspheres were prepared according to a previous literature.[36] Briefly, 5.40 g of $FeCl_3 \cdot 6H_2O$ were dissolved in 200 mL of ethylene glycol under magnetic stirring, and then 14.4 g of sodium acetate were added. The obtained homogeneous yellow solution was transferred into a Teflon-lined stainless-steel autoclave and sealed to heat at 200°C for 8 h. The obtained black magnetite particles were washed with distilled water and absolute ethanol to remove the residues, and then dried under vacuum at 50°C for 12 h.

Synthesis of Fe_3O_4/PANI Core/Shell Microspheres

The Fe_3O_4/PANI core/shell microspheres were synthesized by an *in situ* polymerization method.[33] In the experiment, 1.5 g of Fe_3O_4 microspheres and the required amount of aniline monomer were dispersed into 100 mL of diluted HCl solution (20 mM) under ultrasonication for 30 min to obtain a uniform suspension. Note that here diluted HCl solution is used to minimize the reaction with Fe_3O_4 microsphere, and protonalized aniline adsorbed on Fe_3O_4 microsphere can reduce the corrosion. The mixture was cooled and mechanically stirred in an ice-water bath for 1 h before adding pre-cooled ammonium persulfate (APS) aqueous solution for oxidative polymerization for 20 h. After polymerization, the products were collected by magnetic separation and re-dispersed in distilled water to purify the final products. This process was repeated at least three times until the water phase after sample collection became colorless. Finally, the products were dried in a vacuum drying cabinet at 50°C for 12 h. Throughout the experiments, the molar ratio of aniline monomer to APS was fixed at 1 : 1.1. The final samples were denoted as S1, S2, S3, S4, S5, and S6, where the amounts of aniline monomer were 0.15, 0.30, 0.45, 0.60, 0.75, and 0.90 g, respectively (designed weight ratios of aniline and Fe_3O_4 at 1 : 10, 2 : 10, 3 : 10, 4 : 10, 5 : 10, and 6 : 10).

Characterization

Powder X-ray diffraction (XRD) data were recorded on an XRD-6000 X-ray diffractometer (Shimadzu) with a Cu $K\alpha$ radiation source (40.0 kV, 30.0 mA). Scanning electron microscopic (SEM) images were obtained on the S-4800 (Hitachi), and the samples were mounted on aluminum studs by using adhesive graphite tape and sputtercoated with gold before analysis. Transmission electron microscopic (TEM) images were obtained on a Tecnai G^2-STWIN operating at an accelerating voltage of 220 kV. The magnetic properties (intrinsic coercivity, saturation, and remanent magnetization) were measured by using a vibrating sample magnetometer (VSM, Lake Shore 7410). The thermogravimetric (TG) analysis was carried out on a SETSYS Evolution TGA (Setaram) in the temperature range of room temperature to 800°C at a heating rate of 10°C min^{-1}. An HP-5783E vector network analyzer was applied to determine the relative permeability and permittivity in the frequency range of 1–18 GHz for the calculation of reflection loss, with an input power level of −7 dBm. A sample containing 50 wt % of the obtained products was pressed into a ring with an outer diameter of 7 mm, an inner diameter of 3 mm, and a thickness of 2 mm for microwave measurement, in which paraffin wax was used as the binder.

RESULTS AND DISCUSSION

As reported,[25,36] Fe_3O_4 microspheres prepared from a solvothermal technique are about 300 nm in diameter with a narrow size distribution (Supporting Information Figure S1), which are actually comprised of many small nanoparticles. Using the as-prepared Fe_3O_4 microspheres as cores, PANI can be uniformly coating on the microspheres during the in situ polymerization to produce Fe_3O_4/PANI hybrid microspheres, where no PANI particles and aggregation are found, as shown in Figure 1. The sizes of the hybrid materials display monotonic increase with more aniline monomers applied in the experiments. In order to better understand the PANI shell thickness of these samples, we removed the Fe_3O_4 cores by strong acid treatment. As shown in the TEM images inset in Figure 1, one can see that PANI shells with thicknesses of about 30, 45, 60, 80, 100, and 120 nm are grown on the Fe_3O_4 cores with designed weight ratios of aniline and Fe_3O_4 at 1 : 10, 2 : 10, 3 : 10, 4 : 10, 5 : 10, and 6 : 10, respectively. This means that with proper control of the experimental conditions and suitable relative ratios of aniline monomers and Fe_3O_4 microspheres, PANI shells can be well fabricated on the cores and the shell thickness can be modulated. However, if more aniline monomers are applied, we only get aggregated bulk materials with many Fe_3O_4 microspheres encapsulated by PANI, but not isolated single core/shell structures (Supporting Information Figure S2).

Thermogravimetric (TG) analysis is an ideal tool to determine the exact amount of PANI in the hybrid, as heating the hybrid materials to a temperature of 800°C in air will produce only Fe_2O_3. From the TG curves in Figure 2, one can see two weight losses due to the removal of adsorbed water (before 100°C) and combustion of PANI (starting at about 350°C), and one weak weight increase region (transformation of Fe_3O_4 to Fe_2O_3) in the temperature range of 100–300°C. As HCl doped PANI can be completely burned in air (Figure 2, inset), the final product will be only Fe_2O_3. Therefore, the amount of PANI in the Fe_3O_4/PANI hybrid microspheres can be calculated by

$$\text{wt\% R} = (1 - \text{wt\% PANI-wt\% water}) \frac{1.5M(Fe_2O_3)}{M(Fe_3O_4)} \quad (1)$$

where wt % *R* is the remaining weight percentage after combustion, and *M* indicates the molecular weight of the compound. It is calculated that the weight percentages of PANI in the hybrid

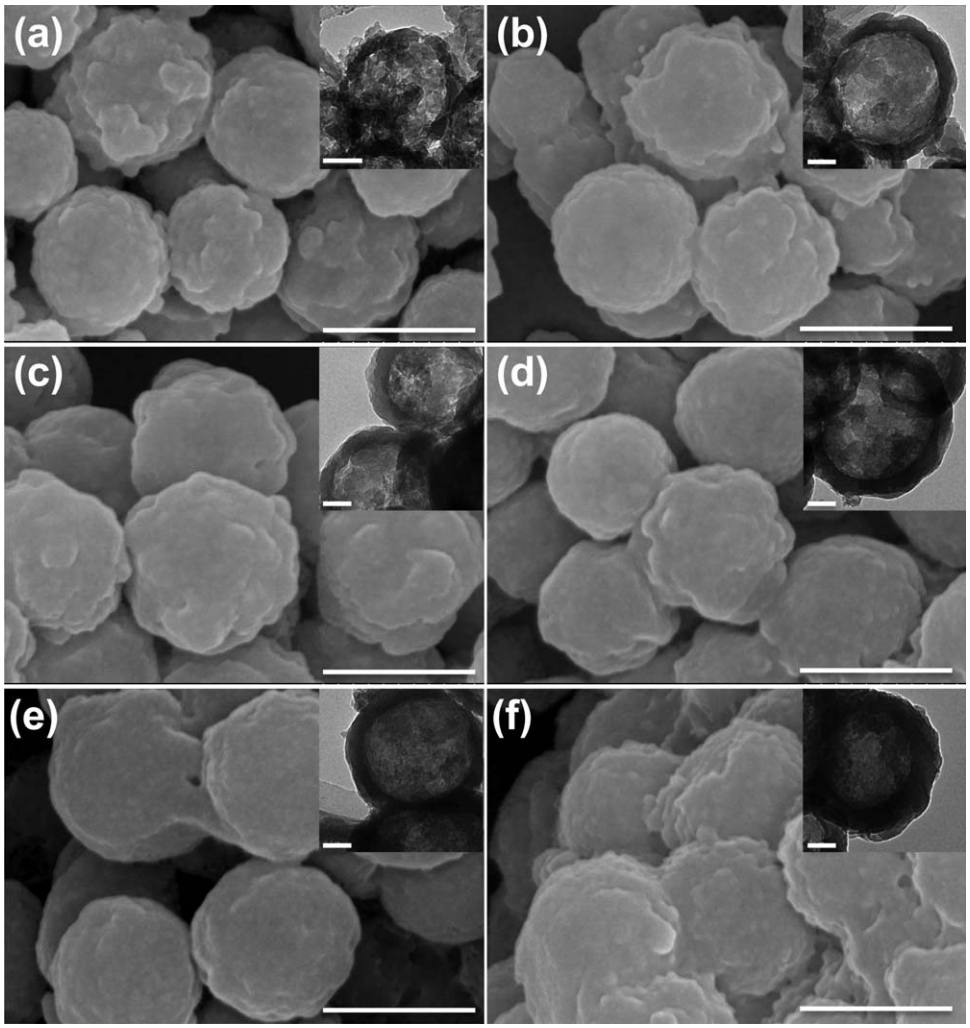

Figure 1. SEM images of the Fe_3O_4/PANI core/shell microspheres with designed weight ratios of aniline and Fe_3O_4 at (a) 1 : 10, (b) 2 : 10, (c) 3 : 10, (d) 4 : 10, (e) 5 : 10, and (f) 6 : 10. Scale bar: 500 nm. Inset in each SEM image is the TEM image showing the thickness of the PANI shell after Fe_3O_4 is removed by acid treatment. Scale bar of TEM images: 100 nm.

materials, with designed weight ratios of aniline and Fe_3O_4 at 1 : 10, 2 : 10, 3 : 10, 4 : 10, 5 : 10, and 6 : 10, are 6.2, 10.6, 14.1, 17.8, 20.7, and 27.5 wt %, respectively (Table I). This indicates that the actual PANI amount in the hybrid materials is somehow lower than that as designed. It can be rationalized by the fact that: (1) water soluble oligomers can inevitably be produced during the polymerization reaction, which can then be removed during the washing procedures; (2) PANI powders without coating on the Fe_3O_4 microspheres can also be formed, which cannot be collected using the magnetic separation technique. Therefore, we get less PANI in the Fe_3O_4/PANI hybrid microspheres, and we see well-dispersed hybrid microspheres from the final products without scattered PANI particles.

Diffraction peaks in the XRD pattern (Figure 3) of the as-prepared Fe_3O_4 microspheres can be well indexed to the (220), (311), (400), (422), (511), (440), and (533) crystal planes of the cubic inverse spinel structure of Fe_3O_4 (JCPDS 19-0629).[19,37] The broadening of the diffraction peaks again verifies that the Fe_3O_4 microspheres, in fact, are assembled from small nanoparticles. PANI has a broad diffraction peak centered at $2\theta = 25°$, which is overwhelmed by the strong diffraction peaks of Fe_3O_4 in the hybrid materials. The diffraction peaks of Fe_3O_4 are all well maintained in the Fe_3O_4/PANI hybrid microspheres, indicating that the crystal structure of Fe_3O_4 is not destroyed during the *in situ* polymerization process. While one can see that the peak intensity of Fe_3O_4 is gradually decreased with the increase in PANI content (shell thickness), which is commonly seen in crystals after a coating process.[38,39]

Figure 4 shows the hysteresis loops of Fe_3O_4 microspheres and Fe_3O_4/PANI core/shell microspheres measured at 300 K. The as-prepared Fe_3O_4 microspheres, with a saturation magnetization (*M*s) of 88.6 emu/g, display a super paramagnetic characteristic, without magnetization and coercivity. This again verifies that the 300 nm Fe_3O_4 microspheres should be assembled by nanoparticles with sizes small than 30 nm.[40] It can be seen that the super paramagnetic property is retained when the Fe_3O_4

Applied Polymer SCIENCE

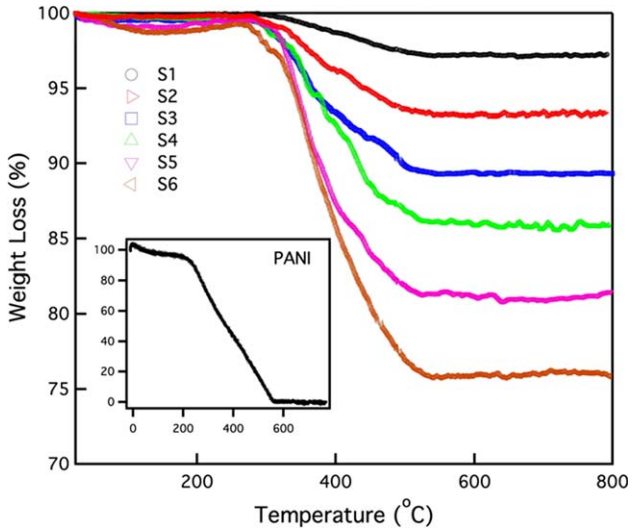

Figure 2. Thermogravimetric (TG) curves of the Fe_3O_4/PANI core/shell microspheres with designed weight ratios of aniline and Fe_3O_4 at (S1) 1 : 10, (S2) 2 : 10, (S3) 3 : 10, (S4) 4 : 10, (S5) 5 : 10, and (S6) 6 : 10, where the actual PANI contents are calculated to be 6.2, 10.6, 14.1, 17.8, 20.7, and 27.5 wt %, respectively. Inset shows the TG curve of HCl-doped PANI. [Color figure can be viewed in the online issue, which is available at wileyonlinelibrary.com.]

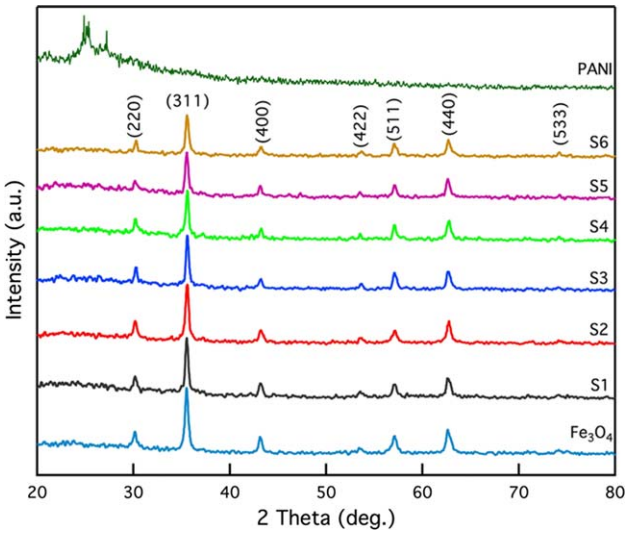

Figure 3. X-ray diffraction (XRD) patterns of PANI, Fe_3O_4 microspheres, and Fe_3O_4/PANI core/shell microspheres with a PANI shell thickness of 30 nm (S1), 45 nm (S2), 60 nm (S3), 80 nm (S4), 100 nm (S5), and 120 nm (S6). [Color figure can be viewed in the online issue, which is available at wileyonlinelibrary.com.]

microspheres are coating with PANI. M_s values of the Fe_3O_4/PANI core/shell microspheres with a PANI shell thickness of 30, 45, 60, 80, 100, and 120 nm are 79.4, 72.8, 67.4, 62.9, 57.8, and 49.0 emu/g, respectively (Table I); namely, the thinner the PANI shells, the stronger the M_s values of the hybrid materials. From the relationship between M_s and PANI content inset in Figure 4, a linear decrease in M_s can be found with the increase in PANI content in the Fe_3O_4/PANI core/shell microspheres, which can be easily understood by the fact that the polymer shell will not affect the magnetic nature of the hybrid materials, but just lower the content of Fe_3O_4. It should be noted here that with increase in the PANI content, the electrical conductivities of the composites are monotonically increased.

According to the transmission line theory, the normalized input impedance Z_{in} of a metal-backed microwave-absorbing layer is given by[24,34,41]

$$Z_{in} = \sqrt{\frac{\mu_r}{\varepsilon_r}} \tanh\left[j\left(\frac{2\pi}{c}\right)\sqrt{\mu_r \varepsilon_r} fd \right] \quad (2)$$

where μ_r and ε_r are the relative permeability and permittivity, respectively, of the composite medium, c is the velocity of electromagnetic waves in free space, f is the frequency of microwaves, and d is the thickness of the absorber. The reflection loss (RL) is related to Z_{in} as

$$\mathrm{RL(dB)} = 20 \log\left| \frac{Z_{in} - 1}{Z_{in} + 1} \right| \quad (3)$$

Table I. Designed Weight Ratio of Aniline and Fe_3O_4, PANI Content From TG Measurement and Saturation Magnetization of Fe_3O_4/PANI Core/Shell Microspheres

Fe_3O_4/PANI Sample	Designed weight ratio of aniline and Fe_3O_4	PANI content from TG measurement (wt %)	Saturation magnetization Ms (emu/g)
S1	1:10	6.2	79.4
S2	2:10	10.6	72.8
S3	3:10	14.1	67.4
S4	4:10	17.8	62.9
S5	5:10	20.7	57.8
S6	6:10	27.5	49.0

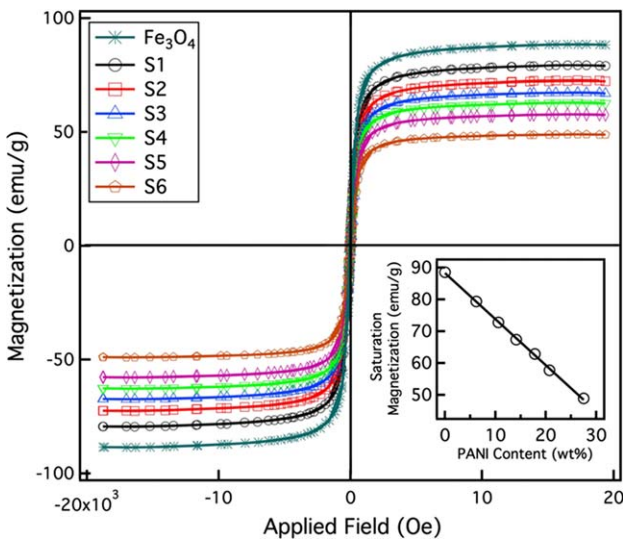

Figure 4. Magnetic properties of Fe_3O_4 microspheres and Fe_3O_4/PANI core/shell microspheres with a PANI shell thickness of 30 nm (S1), 45 nm (S2), 60 nm (S3), 80 nm (S4), 100 nm (S5), and 120 nm (S6). Inset shows the relationship between saturation magnetization and PANI content in the hybrid microspheres. [Color figure can be viewed in the online issue, which is available at wileyonlinelibrary.com.]

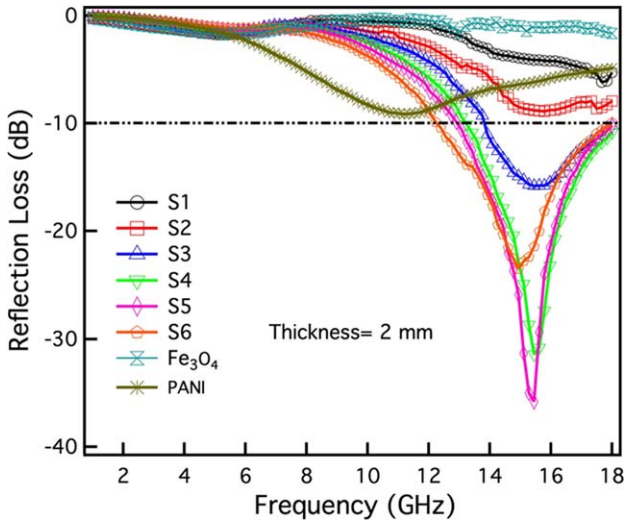

Figure 5. Microwave absorption properties (thickness = 2 mm) of Fe_3O_4, PANI, and Fe_3O_4/PANI core/shell microspheres with a PANI shell thickness of 30 nm (S1), 45 nm (S2), 60 nm (S3), 80 nm (S4), 100 nm (S5), and 120 nm (S6). [Color figure can be viewed in the online issue, which is available at wileyonlinelibrary.com.]

Figure 5 shows the RL values of Fe_3O_4, PANI, and Fe_3O_4/PANI core/shell microspheres in the frequency range of 1–18 GHz, with a thickness of 2 mm. Fe_3O_4 microspheres barely have any microwave absorption in the GHz region, with a maximum RL of −1 dB at about 5.6 GHz. As reported,[25] conducting polymers themselves can be microwave absorbers due to their intrinsic dielectric loss properties. Here, the as-prepared PANI does show some reflection loss in the GHz range, but the RL values are all above −10 dB in the whole frequency range of 1–18 GHz, with a maximum of −9.6 dB at 11.4 GHz, which is not enough as a strong microwave absorber. However, when Fe_3O_4 microspheres are coated with PANI of different shell thicknesses, the microwave absorption behaviors are greatly altered, and the PANI amount (shell thickness) is critical to the microwave absorption abilities of the hybrid materials. Since Fe_3O_4 microspheres only have negligible RL values, introduction of PANI can more or less bring enhanced RL values for all Fe_3O_4/PANI core/shell microspheres. The microwave absorption performances of the hybrid materials are therefore compared to that of pure PANI. With limited amount of PANI (S1 and S2 in Figure 5), no absorption enhancement can be observed (RL values are above −10 dB), but the absorption band is shifted to higher frequency ranges. When the PANI content is higher than 14% (shell thickness larger than 60 nm), as samples S3–S6, one can see RL values below −10 dB. Notably, the maximum RL value is largely dependent on the PANI shell thickness, which increases from −17.2 (15.6 GHz), −32.5 (15.6 GHz), to −37.4 dB (15.4 GHz) when the shell thickness is 60, 80, and 100 nm, respectively. RL values above −30 dB are rarely reported in Fe_3O_4 based composites.[20,23] However, with even more PANI (shell thickness of 120 nm), the maximum RL value is actually decreased to −24.7 dB at 14.8 GHz. This means introduction of proper amount of PANI can enhance the microwave absorption of the Fe_3O_4/PANI hybrid microspheres, but too much PANI will then decrease the microwave absorption. Unfortunately, these composites only perform well at a narrow frequency region, which however may be appealing where strong microwave absorption at a specific frequency is required.

Taking the sample with the largest maximum RL values (S5, shell thickness of 100 nm) for example, the thickness dependent microwave absorption behaviors are studied. In Figure 6, the position of the maximum RL shifts to lower frequencies with increased thickness of the absorber. It is worth noting that a maximum RL below −20 dB can be obtained from all thicknesses except for 1.5 mm, which means the as-prepared Fe_3O_4/PANI hybrid microspheres with a PANI shell thickness of 100 nm can be a highly efficient microwave absorber in various frequency bands simply by adjusting the thickness.

In order to better understand the microwave absorption mechanisms of the Fe_3O_4/PANI core/shell hybrid microspheres, the two important electromagnetic parameters for microwave absorbers, complex permittivity [real (ε') and imaginary (ε'') parts] and permeability [real (μ') and imaginary (μ'') parts], are plotted as a function of frequency in Figure 7. PANI has very high complex permittivity and an obvious frequency dispersion (both ε' and ε'') in the whole frequency range of 1–18 GHz, where ε' decreases from 31.2 at 1 GHz to 9.5 at 18 GHz, and ε'' decreases from 37.1 at 1 GHz to 8.3 at 18 GHz. This high complex permittivity responds to the dielectric loss properties of PANI. As for the Fe_3O_4 microspheres, ε' stabilizes at about 6 in 1–18 GHz, and ε'' almost keeps constant at about 0.1. From the magnified insets, one can see very weak fluctuations. When the Fe_3O_4 microspheres are coated with PANI, both the ε' and ε'' are increased, and more PANI content leads to higher ε' and ε'' values. It should be noted that the frequency dispersion behavior could be maintained in the Fe_3O_4/PANI hybrid materials. PANI has almost constant μ' values at 1 with small fluctuations, while very limited μ' (~0) in the whole frequency range. μ' of

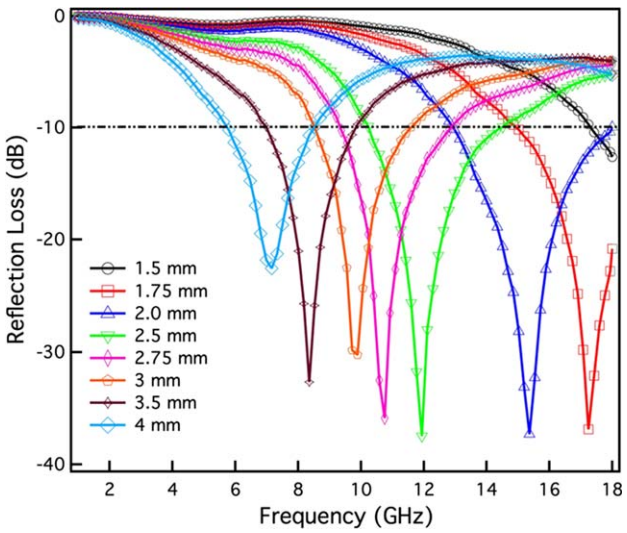

Figure 6. Thickness dependent microwave absorption properties of Fe_3O_4/PANI core/shell microspheres with a PANI shell thickness of 100 nm (S5). [Color figure can be viewed in the online issue, which is available at wileyonlinelibrary.com.]

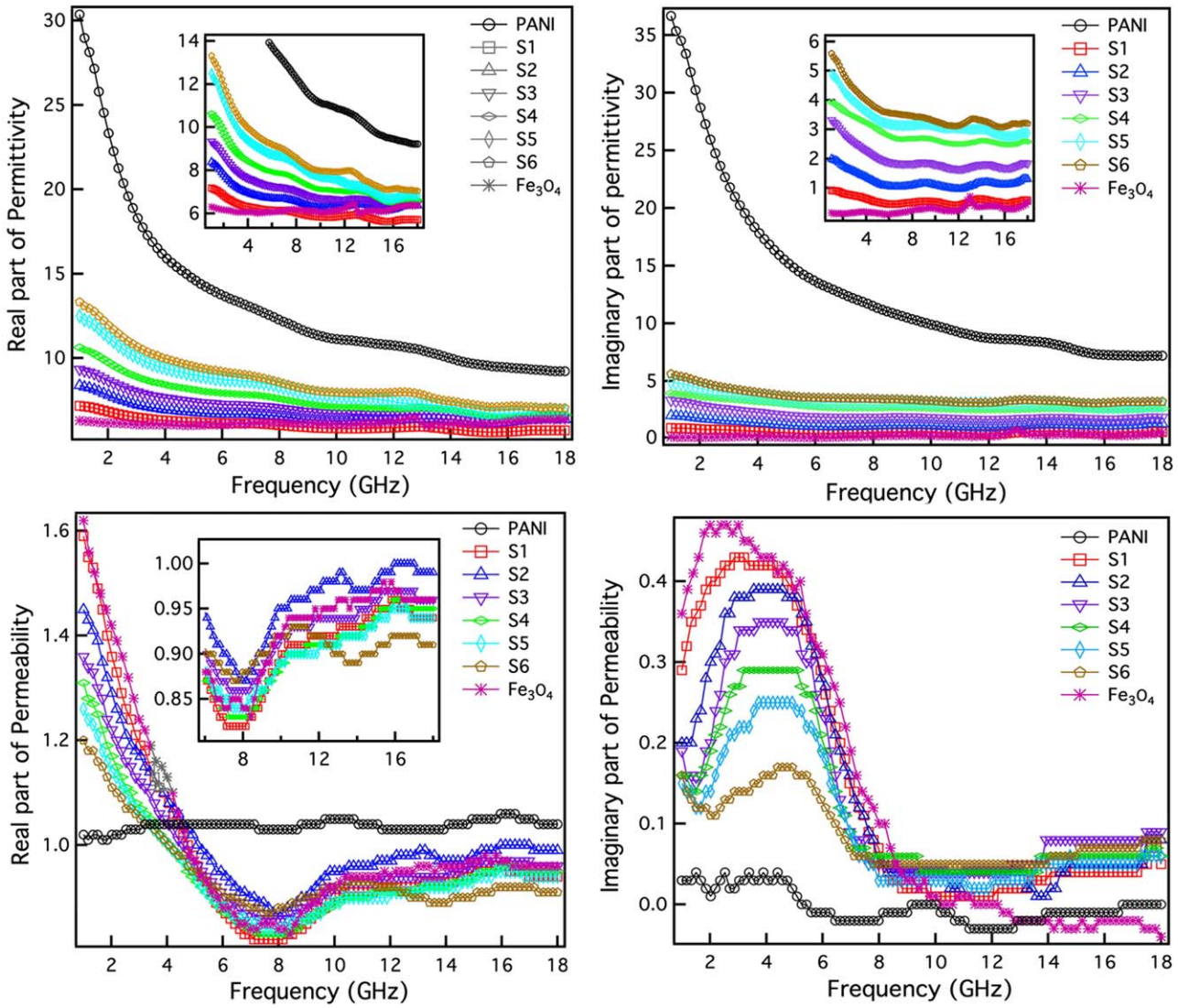

Figure 7. Real and imaginary part of permittivity and permeability of Fe_3O_4, PANI, and Fe_3O_4/PANI core/shell microspheres with a PANI shell thickness of 30 nm (S1), 45 nm (S2), 60 nm (S3), 80 nm (S4), 100 nm (S5), and 120 nm (S6). [Color figure can be viewed in the online issue, which is available at wileyonlinelibrary.com.]

Fe_3O_4 microspheres decreases sharply from 1.63 at 1 GHz to 0.83 at 7.6 GHz, and then gradually increases to 0.95 at 18 GHz. While μ'' increases from 0.36 at 1 GHz to a maximum of about 0.5 at 3 GHz, which then sharply decreases to 0 at 10 GHz then keep negative in 10–18 GHz. It can be seen that complex permeabilities of Fe_3O_4/PANI materials display the same trend as that of Fe_3O_4. μ' of Fe_3O_4/PANI decreases with increasing PANI content in 1–4 GHz, which then becomes irregular. μ'' is also becoming smaller with more PANI in 1–8 GHz, and then turns irregular again. Of note is that all Fe_3O_4/PANI hybrid materials have higher μ'' values in 10–18 GHz. As can be learned, coating Fe_3O_4 microspheres with PANI obviously introduce proper dielectric loss to the hybrid materials, while with the magnetic loss being kept at some level. Enhanced microwave absorption of core/shell structures has been reported due to the lag of polarization between the core/shell interfaces,[42] and here there also should be an interfacial relaxation between the Fe_3O_4 cores and PANI shells. That is to say, interfacial loss should also respond to the enhanced microwave absorption of our core/shell hybrid materials. As can be seen from the transmission line theory, besides the complex permittivity and permeability, another important parameter relating to the RL is the input impedance. Ideally, the characteristic impedance of one absorbing material should be equal to that of free space in order to achieve zero reflection at the front surface of the material. Though Fe_3O_4 microspheres have decent magnetic loss, too small permittivity makes the impedance far away from matching that of the free space, thus very limited RL can be obtained. PANI coating not only provides proper dielectric loss, but also improves the characteristic impedance of the Fe_3O_4/PANI hybrid materials. As can be seen from the input impedance derived from eq. ((3)), introduction of PANI does lead to

improved matching impedance in the hybrid materials (Supporting Information Figure S3). However, too much PANI will lead to high electrical conductivity and permittivity (microwaves are reflected back instead of absorbed), and deteriorated impedance matching, and thus microwave absorption will be decreased again.

CONCLUSIONS

With Fe_3O_4 microspheres as the cores and nucleation sites, core/shell Fe_3O_4/PANI hybrid materials have been prepared via an *in situ* polymerization technique. The shell thickness can be well controlled by modulating the weight ratios of aniline monomers and Fe_3O_4 microspheres. The super paramagnetism of Fe_3O_4 microspheres that are actually comprised of small nanoparticles can be maintained in the prepared Fe_3O_4/PANI hybrid materials, while the saturation magnetization displays a linear decrease with increased PANI content (shell thickness). Fe_3O_4/PANI hybrid materials show enhanced microwave absorption properties, due to the introduction of dielectric loss, interfacial loss, and improved matching impedance after PANI coating. A maximum reflection loss of −37.4 dB has been reached with a 100 nm PANI shell on the Fe_3O_4 microspheres, which is rarely seen in previous reports. Moreover, the responsive frequency band can be modulated by adjusting the thickness of the absorbers. We believe the as-prepared Fe_3O_4/PANI hybrid materials can be promising candidates as strong microwave absorbers.

ACKNOWLEDGMENTS

The authors thank the support from the China Post-doctoral Fund, Natural Science Foundation of China (No. 21003029, 21101041, 21203045, 21071037, and 91122002), Fundamental Research Funds for the Central Universities (Grant No. HIT. NSRIF 2010065, 2011017, and HIT.BRETIII.201223), Innovation Foundation for Young Scientist of Harbin (2011RFXYG021, 2012RFQYG117), and Special Fund of Harbin Technological Innovation (2010RFXXG012).

REFERENCES

1. Li, N.; Huang, Y.; Du, F.; He, X. B.; Lin, X.; Gao, H. J.; Ma, Y. F.; Li, F. F.; Chen, Y. S.; Eklund, P. C. *Nano Lett.* **2006**, *6*, 1141.
2. Yang, Y. L.; Gupta, M. C. *Nano Lett.* **2005**, *5*, 2131.
3. Abbas, S. M.; Chatterjee, R.; Dixit, A. K.; Kumar, A. V. R.; Goel, T. C. *J. Appl. Phys.* **2007**, *101*, 074105.
4. Li, G.; Xie, T. S.; Yang, S. L.; Jin, J. H.; Jiang, J. M. *J. Phys. Chem. C* **2012**, *116*, 9196.
5. Che, R. C.; Peng, L. M.; Duan, X. F.; Chen, Q.; Liang, X. L. *Adv. Mater.* **2004**, *16*, 401.
6. Liu, J. W.; Xu, J. J.; Che, R. C.; Chen, H. J.; Liu, Z. W.; Xia, F. *J. Mater. Chem.* **2012**, *22*, 9277.
7. Xia, F.; Liu, J. W.; Gu, D.; Zhao, P. F.; Zhang, J.; Che, R. C. *Nanoscale* **2011**, *3*, 3860.
8. Du, L.; Du, Y. C.; Li, Y.; Wang, J. Y.; Wang, C.; Wang, X. H.; Xu, P.; Han, X. J. *J. Phys. Chem. C* **2010**, *114*, 19600.
9. Cao, M. H.; Lian, H. Q.; Hu, C. W. *Nanoscale* **2010**, *2*, 2619.
10. Zhang, H. Y.; Zeng, G. X.; Ge, Y.; Chen, T. L.; Hu, L. C. *J. Appl. Phys.* **2009**, *105*, 054314.
11. Zhao, H. T.; Zhang, B.; Zhang, J. S.; Zhang, L. F.; Han, X. J.; Xu, P.; Zhou, Y. *J. Phys. Chem. C* **2010**, *114*, 21214.
12. Wang, C.; Han, X. J.; Zhang, X. L.; Hu, S. R.; Zhang, T.; Wang, J. Y.; Du, Y. C.; Wang, X. H.; Xu, P. *J. Phys. Chem. C* **2010**, *114*, 14826.
13. Wang, C.; Han, X. J.; Xu, P.; Wang, J. Y.; Du, Y. C.; Wang, X. H.; Qin, W.; Zhang, T. *J. Phys. Chem. C* **2010**, *114*, 3196.
14. Zhao, H. T.; Han, X. J.; Zhang, L. F.; Wang, G. Y.; Wang, C.; Li, X. A.; Xu, P. *Radiat. Phys. Chem.* **2011**, *80*, 390.
15. Tung, T. T.; Feller, J. F.; Kim, T.; Kim, H.; Yang, W. S.; Suh, K. S. *J. Polym. Sci. B: Polym. Chem.* **2012**, *50*, 927.
16. Wei, J.; Liu, J. H.; Li, S. M. *J. Magn. Magn. Mater.* **2007**, *312*, 414.
17. Zhao, R.; Jia, K.; Wei, J. J.; Pu, J. X.; Liu, X. B. *Mater. Lett.* **2010**, *64*, 457.
18. Li, X. A.; Zhang, B.; Ju, C. H.; Han, X. J.; Du, Y. C.; Xu, P. *J. Phys. Chem. C* **2011**, *115*, 12350.
19. Liu, J. W.; Che, R. C.; Chen, H. J.; Zhang, F.; Xia, F.; Wu, Q. S.; Wang, M. *Small* **2012**, *8*, 1214.
20. Zhu, C. L.; Zhang, M. L.; Qiao, Y. J.; Xiao, G.; Zhang, F.; Chen, Y. J. *J. Phys. Chem. C* **2010**, *114*, 16229.
21. Chen, Y. J.; Gao, P.; Wang, R. X.; Zhu, C. L.; Wang, L. J.; Cao, M. S.; Jin, H. B. *J. Phys. Chem. C* **2009**, *113*, 10061.
22. Chen, Y. J.; Zhang, F.; Zhao, G. G.; Fang, X. Y.; Jin, H. B.; Gao, P.; Zhu, C. L.; Cao, M. S.; Xiao, G. *J. Phys. Chem. C* **2010**, *114*, 9239.
23. Chen, Y. J.; Gao, P.; Zhu, C. L.; Wang, R. X.; Wang, L. J.; Cao, M. S.; Fang, X. Y. *J. Appl. Phys.* **2009**, *106*, 054303.
24. Chen, K.; Li, X. H.; Lv, D. S.; Yu, F. Y.; Yin, Z. E.; Wu, T. *Mater. Sci. Eng. B Adv.* **2011**, *176*, 1239.
25. Dechanterac, H.; Roduit, P.; Belhadjtahar, N.; Fourrierlamer, A.; Djigo, Y.; Aeiyach, S.; Lacaze, P. C. *Synth. Methods* **1992**, *52*, 183.
26. Joo, J.; Lee, C. Y.; Song, H. G.; Kim, J. W.; Jang, K. S.; Oh, E. J.; Epstein, A. J. *Mol. Cryst. Liquid Cryst A* **1998**, *316*, 367.
27. Jiang, J.; Ai, L. H.; Qin, D. B.; Liu, H.; Li, L. C. *Synth. Methods* **2009**, *159*, 695.
28. Saini, P.; Choudhary, V.; Singh, B. P.; Mathur, R. B.; Dhawan, S. K. *Mater. Chem. Phys.* **2009**, *113*, 919.
29. Zhou, W. C.; Hu, X. J.; Bai, X. X.; Zhou, S. Y.; Sun, C. H.; Yan, J.; Chen, P. *ACS Appl. Mater. Int.* **2011**, *3*, 3839.
30. Zhang, W. D.; Xiao, H. M.; Zhu, L. P.; Fu, S. Y.; Wan, M. X. *J. Polym. Sci. B: Polym. Chem.* **2010**, *48*, 320.
31. Dong, X. L.; Zhang, X. F.; Huang, H.; Zuo, F. *Appl. Phys. Lett.* **2008**, 92.
32. Xu, P.; Han, X. J.; Wang, C.; Zhou, D. H.; Lv, Z. S.; Wen, A. H.; Wang, X. H.; Zhang, B. *J. Phys. Chem. B* **2008**, *112*, 10443.
33. Xu, P.; Han, X. J.; Jiang, J. J.; Wang, X. H.; Li, X. D.; Wen, A. H. *J. Phys. Chem. C* **2007**, *111*, 12603.

34. Xu, P.; Han, X. J.; Wang, C.; Zhao, H. T.; Wang, J. Y.; Wang, X. H.; Zhang, B. *J. Phys. Chem. B* **2008**, *112*, 2775.

35. Saini, P.; Arora, M. Microwave Absorption and EMI Shielding Behavior of Nanocomposites Based on Intrinsically Conducting Polymers, Graphene and Carbon Nanotubes. New Polymers for Special Applications Intech: Croatia, **2012**; p 72.

36. Xu, X. Q.; Deng, C. H.; Gao, M. X.; Yu, W. J.; Yang, P. Y.; Zhang, X. M. *Adv. Mater.* **2006**, *18*, 3289.

37. Liu, X. G.; Or, S. W.; Ho, S. L.; Cheung, C. C.; Leung, C. M.; Han, Z.; Geng, D. Y.; Zhang, Z. D. *J. Alloy Compd.* **2011**, *509*, 9071.

38. Chen, C. T.; Chen, Y. C. *Anal. Chem.* **2005**, *77*, 5912.

39. Luo, Y. S.; Luo, J. S.; Jiang, J.; Zhou, W. W.; Yang, H. P.; Qi, X. Y.; Zhang, H.; Fan, H. J.; Yu, D. Y. W.; Li, C. M.; Yu, T. *Energy Environ. Sci.* **2012**, *5*, 6559.

40. Deng, H.; Li, X. L.; Peng, Q.; Wang, X.; Chen, J. P.; Li, Y. D. *Angew Chem. Int. Ed.* **2005**, *44*, 2782.

41. Singh, P.; Babbar, V. K.; Razdan, A.; Puri, R. K.; Goel, T. C. *J. Appl. Phys.* **2000**, *87*, 4362.

42. Zhang, X. F.; Dong, X. L.; Huang, H.; Liu, Y. Y.; Wang, W. N.; Zhu, X. G.; Lv, B.; Lei, J. P.; Lee, C. G. *Appl. Phys. Lett.* **2006**, *89*, 053115.